scientific reports

Check for updates

OPEN

Optimizing oxytetracycline removal from aqueous solutions using activated carbon from barley lignocellulosic wastes with isotherms and thermodynamic studies

Ali Kazemi[1]✉, Elaheh Ebrahimpour[2], Milad Esmaeilbeigi[3], Farideh Gheitasi[4], Fatemeh Einollahipeer[5] & Mansure Mohammadrezai[6]

The excessive presence of antibiotics such as Oxytetracycline (OTC) in the wastewater has increased health problems due to their toxic impact on the aquatic ecosystem. Therefore, their removal has become an important topic. This study aims to produce high surface area-activated carbon derived from low-cost and environmentally friendly barley lignocellulosic wastes to remove OTC from aqueous solutions. The synthesized barley wastes-activated carbon (BW-AC) was characterized using Fourier-Transform Infrared spectroscopy, Thermal Gravimetric Analysis, X-ray diffraction analysis, N_2 adsorption/desorption isotherms, and Scanning Electron Microscopy. A Central Composite Design under the Response Surface Methodology (CCD-RSM) was applied to optimize the operational parameters (adsorbent dosage, pH, OTC initial concentration, and contact time) affecting the adsorption capacity as the response factor. The optimum condition of OTC adsorption by BW-AC was the adsorbent dosage of 16.25 mg, pH of 8.25, initial concentration of 62.50 mg/L, and contact time of 23.46 min. An analysis of variance (ANOVA) was performed to investigate the significance of the designed quadratic model and evaluate the parameters interactions. The linear regression coefficient (R^2) of 0.975 shows a good correlation between predicted and actual results. The adsorption isotherms were used to determine the contaminant distribution over the adsorbent surface, and the equilibrium data was best described by the Freundlich isotherm due to the R^2 value of 0.99 compared to other isotherms and β parameter of 0.23 in Redlich-Peterson equation. Moreover, the n value of 1.25 in Freundlich equation and E value of 0.31 in Dubinin–Radushkevich equation indicates a physical nature of adsorption process. According to the equations results, the maximum adsorption capacity of BW-AC for OTC removal was 500 mg/g, based on the Langmuir isotherm equation. In addition, the thermodynamic studies indicated an endothermic process based on the 0.31 value of ΔH° and spontaneous nature due to the negative amount of ΔG° within the temperature range of 288–318 K. Consequently, the prepared BW-AC can be deemed as a highly effective adsorbent with a large surface area, resulting in significant capacity for removing OTC. This synthesized BW-AC can serve as an environmentally friendly adsorbent for affordable wastewater treatment and is poised to make valuable contributions to future research in this field.

Keywords Oxytetracycline, Antibiotic, Response surface methodology, Wastewater treatment

[1]Department of Environmental Science and Engineering, Arak University, Arak, Iran. [2]Research and Development Department of Arvin Zist Pooya Lab, Tehran 1563794747, Iran. [3]Centre for Applied Water Science, Institute for Applied Ecology, University of Canberra, Canberra, ACT, Australia. [4] Department of Sustainable Development, Environmental Science and Engineering (SEED), KTH Royal Institute of Technology, Stockholm, Sweden. [5]Department of Environment, Faculty of Natural Resources, University of Zabol, Zabol, Sistan and Baluchestan, Iran. [6]Department of Civil and Environmental Engineering, Payame Noor University, Tehran, Iran. ✉email: kazemi@rocketmail.com; a-kazemi64@araku.ac.ir

Antibiotics are antimicrobial chemicals that destroy bacteria and inhibit the metabolic activities of microorganisms[1]. These powerful chemicals are used to effectively treat infections and are commonly prescribed as medicine for humans and growth promoters for animals. In fact, approximately 15% of all medications worldwide are dedicated to antibiotics[2,3]. The widespread use of antibiotics as medication, along with their incomplete metabolization after consumption and their extended presence in the environment, has led to their emergence as a significant potential pollutant in ecosystems over the past few decades[4–6]. They can enter into water sources from various points of origin including pharmaceutical industries, veterinary clinics, Wastewater Treatment Plants (WWTPs), chemical industrial plants, crop husbandry and aquaculture[7–9]. Due to the resistant nature of antibiotics residues, they accumulate to higher concentrations in groundwater, wastewater and marine environments[10–12]. They can also cause contamination in solids such as manure-amended soil, river sediment and sludge due to their high stability and biological activity[13–17]. These pharmaceuticals have been shown to be harmful to both animal and human health by making more resistant pathogens to drugs that can be transmitted to populations, and may also have a toxic effect on various microorganismal clusters[18–20]. One of the most common and widely used antibiotics is OTC, a broad-spectrum and low-cost antibiotic additive that restrains the synthesis of bacteria protein by blocking the attachment of aminoacyl-tRNA units to control bacterial infections[21]. It belongs to the tetracycline family and is used to improve aquaculture and livestock growth as one of the main veterinary medicinal products[22,23]. However, OTCs medications contribute to health issues by increasing the microbial resistance in certain microorganisms, ultimately diminishing the effectiveness of antibiotics. Additionally, these drugs may pose potential risks such as teratogenic effects during pregnancy, impact on the immune system, inhibition or reduction of catalase, and effects on avian cartilage degradation[24,25]. These toxic medications enter and pollute the environment by contaminating soil, sewage treatment plants and marine sediments[26]. Aga et al.[27]. studied the persistence of tetracycline family and found that OTC is the most persistent tetracycline in subsurface soils after several months of incubation. Considering the extensive use of OTC, their potential harm to both humans and animals, as well as their resistance in the environment, particularly in aqueous settings, it is important to investigate adaptive treatments to remove OTC from wastewater and industrial effluents. Various methods have been proposed for efficient OTC removal from aqueous solutions. These include oxidation, adsorption, enzymatic degradation, photochemical degradation and electrocoagulation[28–31]. Due to the stable naphthol ring in the antibiotic structure, it is difficult to use the biodegradation method, and the toxicity of OTC to microorganisms make it hard to use antibiotic degradation. In addition, some degradation byproducts have proven to be more toxic than their compounds[32,33]. However, among these numerous methods, the adsorption process is an especially effective method because of its adsorbent recovery, cost-effectiveness, process simplicity, prevention of making secondary pollutants, and safety[34–36]. In the group of adsorbents that have been studied for antibiotics removal, activated carbon is very common because of its high surface area, functional groups and high capacity[37,38]. However, the extensive usage of activated carbon as a contaminant remover leads to its high price and, as a result, formulating high-quality activated carbon at low cost has become a major issue. A wide variety of carbonaceous substances can be suitable for activated carbon preparation, so natural adsorbents produced at lower prices have been used as efficient pollutant removers[39]. The chemical and textual characteristics of activated carbon depend on the nature of the pioneer substance and the production process. Natural adsorbents are not harmful to the ecosystem and have been investigated in many studies such as the application of walnut shell[40], Nasturtium officinale[41], cotton stalks[31], oil palm shell[42], and hazelnut[43]. Barley lignocellulosic wastes can provide a low-cost raw material for activated carbon production and is an agricultural waste that is produced annually in large amounts. Barley wastes conversion to activated carbon is economically valuable due to the cost reduction of waste disposal and ecologically valuable because of its agricultural nature. As far as we know, no study has been performed to evaluate the performance of BW-AC for OTC removal. This study has been carried out to prepare a novel, low-cost, and environmental-friendly adsorbent with high surface area and capacity for effective adsorption of OTC from aqueous systems. In most studies, application of conventional methods ends in spending more money, time, and chemicals because of the big sample size[44,45]. However, new statistical techniques have been found to be more effective and simpler for optimization of the process[2]. In order to investigate the parameters effects on the efficiency of OTC removal from aqueous solutions, a series of experiments were designed using CCD-RSM. This method is one of the best analytical methods to decide about the effects of parameters on the response factors and interaction of the parameters, with a reasonable number of trials[36,46]. BW-AC was characterized using different methods to best investigate the adsorbent properties. Furthermore, various adsorption isotherm models were applied to estimate the adsorption capacity of the prepared adsorbent. In addition, thermodynamics studies were accomplished to better understand the nature of the adsorption process.

Reagents, material characterization, and methods

Reagents

Pure standard of OTC 95% was obtained from Sigma-Aldrich (Pvt. Ltd., USA). All other chemicals including potassium hydroxide (KOH), hydrochloric acid 37% (HCl), and Sodium hydroxide (NaOH) were purchased from Merck (KGaA, Darmstadt, Germany). Deionized (DI) water was used for preparation of all the aqueous solutions in preparation and adsorption processes. All the chemicals were of analytical-reagent grade and applied directly without further purification.

Methods

The activated carbon was prepared from barley lignocellulosic wastes provided from a malt beverage factory. The procedure of activated carbon preparation and the OTC removal using the volumetric method is depicted schematically in Fig. 1. For preparation of the activated carbon, firstly the barley lignocellulosic wastes were sieved through a 60 mesh (<0.25 mm) and then oven-dried at the temperature of 110 °C for 24 h. Afterward,

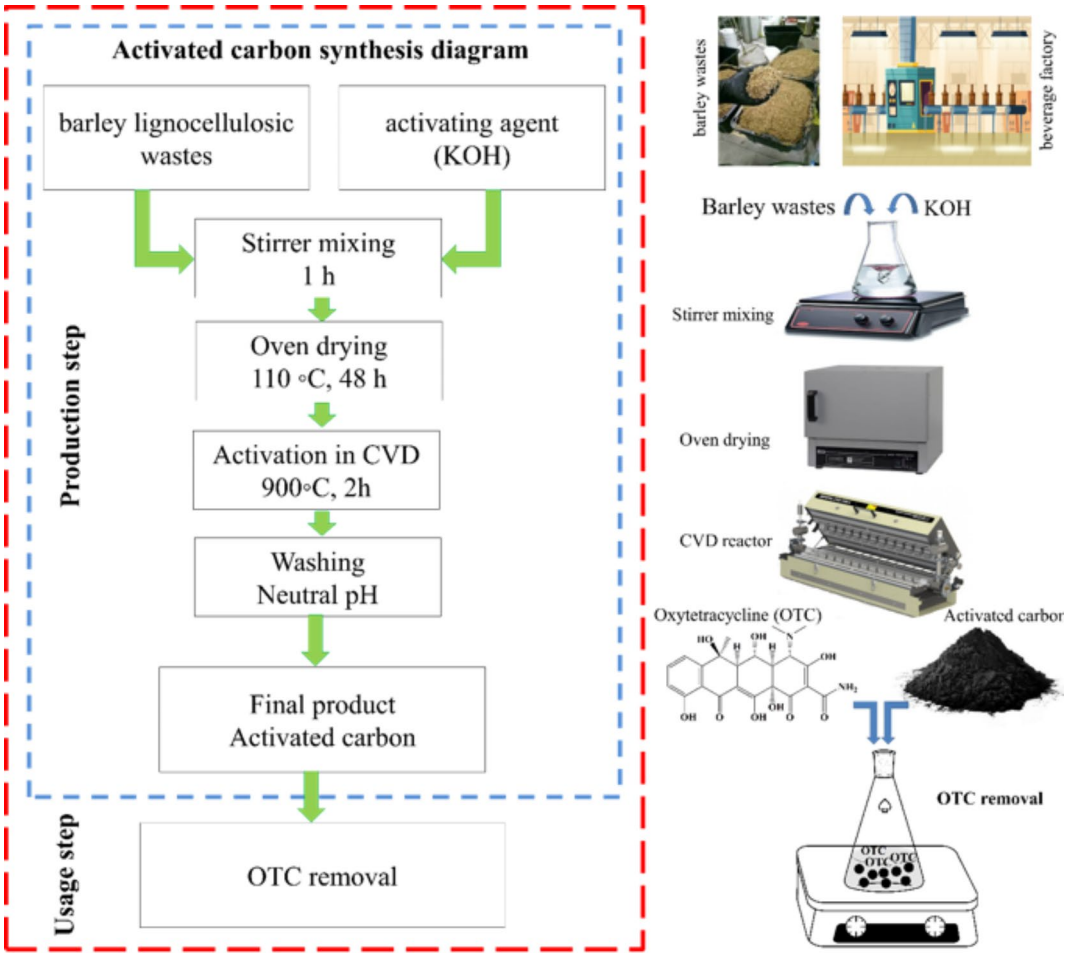

Fig. 1. The schematic diagram of activated carbon synthesis and OTC removal procedure.

KOH was used as an activating agent at the mass ratio of precursor to activating agent equal to 1:3 g/g. The precursor and activating agent were mixed and stirred continuously at ambient temperature for 1 h to complete the reaction and then dried in the oven at temperature of 110 °C for 48 h. The pyrolysis process was carried out under N_2 atmosphere flow (100 mL/min) in the quartz reactor of a stationary horizontal stainless-steel tube furnace (CVD reactor) at 900 °C for 2 h. After the activation time, the prepared sample was cooled in an N_2 atmosphere and then removed from the CVD reactor. Afterward, the pyrolysis product was washed several times with DI water until the wash water reached a neutral pH, then it dried at a temperature of 110 °C for 24 h.

Material characterization

The functional groups of prepared compounds were identified by a Thermo Scientific Nicolet IR100 Fourier-transform infrared (FTIR) spectrometer on KBr pallets over the wavenumber range of 4000 to 400 cm^{-1}. The X-Ray (XRD) Diffraction pattern was determined by a Philips X-Pert 1710 diffractometer with Cu Kα radiation (λ = 1.54056 Å, voltage: 40 kV, current: 40 mA) between 5° and 80° (2θ) at an angular speed of 0.05°/s and ambient temperature. Thermogravimetric Analysis (TGA) of BW-AC was accomplished by a Mettler Toledo AG—TGA/SDTA851e under the N_2 atmosphere with a heating rate of 10 °C min^{-1} and in the range of 25–900 °C. The textural properties of the synthesized compounds were characterized using a N_2 adsorption isotherm at 77 K with a Micromeritics ASAP 2020 nitrogen adsorption apparatus (the synthesized activated carbon was degassed under vacuum for about 12 h at 100 °C before the adsorption measurements). The Brunauer–Emmett–Teller (BET) and the Brunauer–Joyner–Hallenda (BJH) methods were used to determine specific surface area and pore size distribution. Finally, TESCAN MIRA FE field emission scanning electron microscopy (SEM) on a gold-coated sample was used to investigate the surface morphology of the prepared activated carbon, and the concentration of OTC was determined by a Unico 2100 UV–Visible spectrophotometer.

Batch adsorption procedure

Adsorption experiments were conducted using the batch experimental system. Stock solutions were prepared by dissolving OTC in DI water in a concentration range of the designed model and the calibration curve was plotted. The adsorption trials were designed by CCD-RSM to optimize the different parameters affecting the adsorption capacity. Those parameters included initial concentration (C_0, mg/L), initial pH, adsorbent dosage (m, mg) and

contact time (t, min.). Initially, a certain dosage of BW-AC was added into 100 ml of OTC solutions with a certain initial concentration. Then the pH value was adjusted using 0.1 M NaOH and 0.1 M HCl solutions. All the batch trials were performed on a magnetic stirrer at 25 ℃ with an agitation speed of 700 rpm. After equilibrium was reached, the adsorbent was separated by filtration and the supernatant was collected for measurement of the un-adsorbed OTC in the solutions at 355 nm using a UV–Visible spectrophotometer. The amount of adsorbed OTC antibiotic per unit mass of BW-AC adsorbent (the adsorption capacity) was calculated from Eq. (1).

$$q_e\,(mg/g) = ((C_0 - C_e) \times V)\,/W \tag{1}$$

where q_e is the adsorption capacity of the prepared adsorbent (mg/g), W is the adsorbent weight (g), V is the solution volume (ml), and C_e and C_0 are the equilibrium and initial concentrations of the adsorbed antibiotic (mg/L), respectively.

Experimental design by CCD

The optimization of vital parameters affecting the adsorption capacity of BW-AC for OTC adsorption was accomplished by the CCD-RSM. This experimental design is an efficient technique for modeling the process, reducing the number of trials, and investigation of different parameters interactions[47,48]. CCD-RSM was applied to enhance the adsorption capacity and optimize the independent parameters including solution pH, adsorbent dosage, OTC initial concentration, and contact time. The linear, interactive, and quadratic effects of these parameters were investigated as the affecting factors at four levels. Moreover, the adsorption capacity of OTC was considered as the response factor. Table 1 indicates the levels and coded values of the four independent parameters.

As seen in Table 2, a total of 30 experiments with six central points was designed to study the effect of the parameters on the response factor based on the quadratic model. All experiments were carried out thrice and the adsorbed concentrations given in Table 2 were the means of triplicate experimental results. After developing the experiments, a second-order polynomial model (Eq. 2) was used to correlate the response factor and independent parameters, and predict the optimal conditions of the OTC adsorption process:

$$\mathrm{Y} = \beta_0 \sum_{\mathrm{i}=1}^{\mathrm{n}} \mathrm{a_i x_i} + \sum_{\mathrm{i}=1}^{\mathrm{n}} \mathrm{a_{ii} x_i^2} + \sum_{\mathrm{i}=1}^{\mathrm{n}-1} \sum_{\mathrm{j}=2}^{\mathrm{n}} \mathrm{a_{ij} x_i x_j} + \varepsilon \tag{2}$$

where Y is the predicted response factor, β_0 is the constant coefficient, $\mathrm{x_i}$ and $\mathrm{x_j}$ indicate the independent parameters in the form of coded values, $\mathrm{a_i}$, $\mathrm{a_{ii}}$ and $\mathrm{a_{ij}}$ are the regression coefficients, and ε is the random error. The CCD experimental design and statistical analysis were performed using Statgraphics software, version 19.

Results and discussion

Characteristics of prepared activated carbon

FTIR spectroscopy is a useful and qualitative method for characterizing functional groups of materials and investigating the adsorption process by measuring the changes of vibration frequencies[49]. According to the chemical structure that was analyzed by FTIR spectroscopy (Fig. 2a), the absorption band observed at 3419 cm^{-1} represents the stretching vibration of the hydroxyl functional groups. The absorption band observed at 2921 cm^{-1} indicates the stretching and bending vibration of C–H in the $-CH_2$ groups. Moreover, the peaks at 1636 cm^{-1} and 1384 cm^{-1} correspond to the –OH bending vibrations of H_2O molecules. Also, the strong absorption band at 1070 cm^{-1} is attributed to the axial deformation vibrations of the C–N bond of aliphatic amines. The TGA of BW-AC in a nitrogen atmosphere was carried out to find the maximal degradation temperature. The TGA curve indicates different stages of weight loss (Fig. 2b). The first weight reduction occurs at approximately 100 °C because of residual moisture evaporation, and also because of the thermal desorption of hydrocarbons[50]. A second peak of weight loss was observed at near 550°C which was related to the activated carbon oxidetion[51]. Overall, it can be concluded that the activation process of carbon improves the synthesized adsorbent stability to the temperature and also excel the matrix for a more efficient adsorption. The XRD pattern of BW-AC in the range of 2θ = 5°–80° is presented in Fig. 2c. Two broad bands are exhibited around 2θ = 23° and 44° relating to (0 0 2) and (1 0 0) planes, respectively. These diffraction bands represent an amorphous and disordered structure of activated carbon and also the existence of coherent layers of carbon sheets[52]. The adsorption–desorption of inert gases such as $N_2$is a common method for determination of the adsorbents pore structure[53]. The N_2 adsorption–desorption isotherm of activated carbon at 77 K, synthesized from Barley wastes

Independent variables	Symbol	Unit	Levels			
Adsorbent dosage	A	mg	5.00	16.25	27.50	38.75
pH	B	–	3.00	4.75	6.50	8.25
Initial concentration	C	mg/L	27.50	45.00	62.50	80.00
Contact time	D	min	22.50	35.00	47.50	60.00

Table 1. The levels of independent variables in the experimental design.

Run	Adsorbent dosage (mg)	pH	Initial concentration (mg/L)	Contact time (min)	Adsorption capacity (actual)	Adsorption capacity (predicted)
1	27.50	6.50	80.00	35.00	74.48	87.59
2	27.50	6.50	45.00	60.00	25.40	26.64
3	38.75	4.75	62.50	47.50	8.48	0.18
4	38.75	8.25	62.50	47.50	88.07	85.26
5	27.50	6.50	45.00	35.00	30.65	40.26
6	27.50	6.50	45.00	35.00	35.32	40.26
7	50.00	6.50	45.00	35.00	71.29	72.67
8	38.75	4.75	27.50	22.50	34.79	45.86
9	38.75	8.25	62.50	22.50	93.64	94.65
10	38.75	4.75	62.50	22.50	17.49	13.09
11	16.25	8.25	27.50	47.50	41.96	46.08
12	16.25	4.75	62.50	22.50	42.95	48.77
13	16.25	4.75	27.50	47.50	30.77	31.90
14	16.25	8.25	27.50	22.50	32.61	43.05
15	16.25	4.75	62.50	47.50	31.63	37.31
16	27.50	3.00	45.00	35.00	4.62	−7.30
17	27.50	6.50	45.00	35.00	46.75	40.26
18	38.75	8.25	27.50	47.50	5.90	2.22
19	16.25	8.25	62.50	22.50	198.68	186.24
20	38.75	4.75	27.50	47.50	31.77	43.93
21	27.50	6.50	45.00	35.00	39.48	40.26
22	27.50	6.50	10.00	35.00	3.12	−11.85
23	27.50	6.50	45.00	10.00	39.62	36.51
24	16.25	4.75	27.50	22.50	29.85	32.38
25	27.50	6.50	45.00	35.00	38.96	40.26
26	27.50	10.00	45.00	35.00	78.39	88.45
27	27.50	6.50	45.00	35.00	50.39	40.26
28	5.00	6.50	45.00	35.00	155.47	152.22
29	16.25	8.25	62.50	47.50	187.23	178.30
30	38.75	8.25	27.50	22.50	6.58	0.62

Table 2. Experimental design in CCD for OTC adsorption capacity.

by KOH activation, is displayed in Fig. 3. According to the IUPAC classification[54], the prepared activated carbon demonstrates a combination of Type I and IV isotherm and hysteresis loop at P/P0 > 0.4, which indicates the growth of mesopores. However, micropores are still dominated in the structure of ACs, moving toward a Type IV isotherm[55]. The textural properties of the AC, including specific surface area, mean pore diameter, and pore volume are given in Table 3. The BET results show that the specific surface area of BW-AC was 903.07 m^2/g which is high compared to prepared activated carbons in similar studies (Table 3). The surface morphology of the adsorbent was evaluated by SEM technique which is highly developed in recent years that results in providing more in-depth analysis[56]. Figure 4a and b present the SEM micrographs of a porous activated carbon surface at 100 and 25 Kx magnification, respectively. The SEM micrographs indicated plenty of activated sites on the external surface of BW-AC and inter-particle voids on a heterogeneous structure of the adsorbent which would be positively impact the adsorbent capacity. It should be noted that the exact pore size distribution and pore volume of prepared activated carbon was determined by the analysis of N_2 adsorption isotherm, which proves that the produced activated carbon has a significant high surface area.

Statistical analysis of OTC adsorption with BW-AC

The statistical analysis was completed to study the interactive effects of independent parameters including pH, contact time, adsorbent dosage and initial concentration affecting the adsorption process of OTC using BW-AC in aqueous solutions. To optimize the parameters, 30 experiments were designed by CCD model outlined in Table 2. The highest and the lowest BW-AC capacities for OTC adsorption were around 199 and 3 (mg/g), respectively. Moreover, the equation of the quadratic model in the form of a second-order polynomial describes the interaction between the response factor and the studied parameters. This Equation describes the system behavior generally:

$$\begin{aligned} q_e = {} & 111.175 - 4.22674\,(A) - 3.95746\,(B) - 2.87147\,(C) + 1.30743\,(D) + 0.176338\left(A^2\right) \\ & - 0.709907\,(AB) + -0.0624325\,(AC) - 0.00256853\,(AD) - 0.906322\left(B^2\right) + 1.03511\,(BC) \\ & + 0.0402275\,(BD) - 0.00311077\left(C^2\right) - 0.0125491\,(CD) - 0.0161565\left(D^2\right) \end{aligned} \quad (3)$$

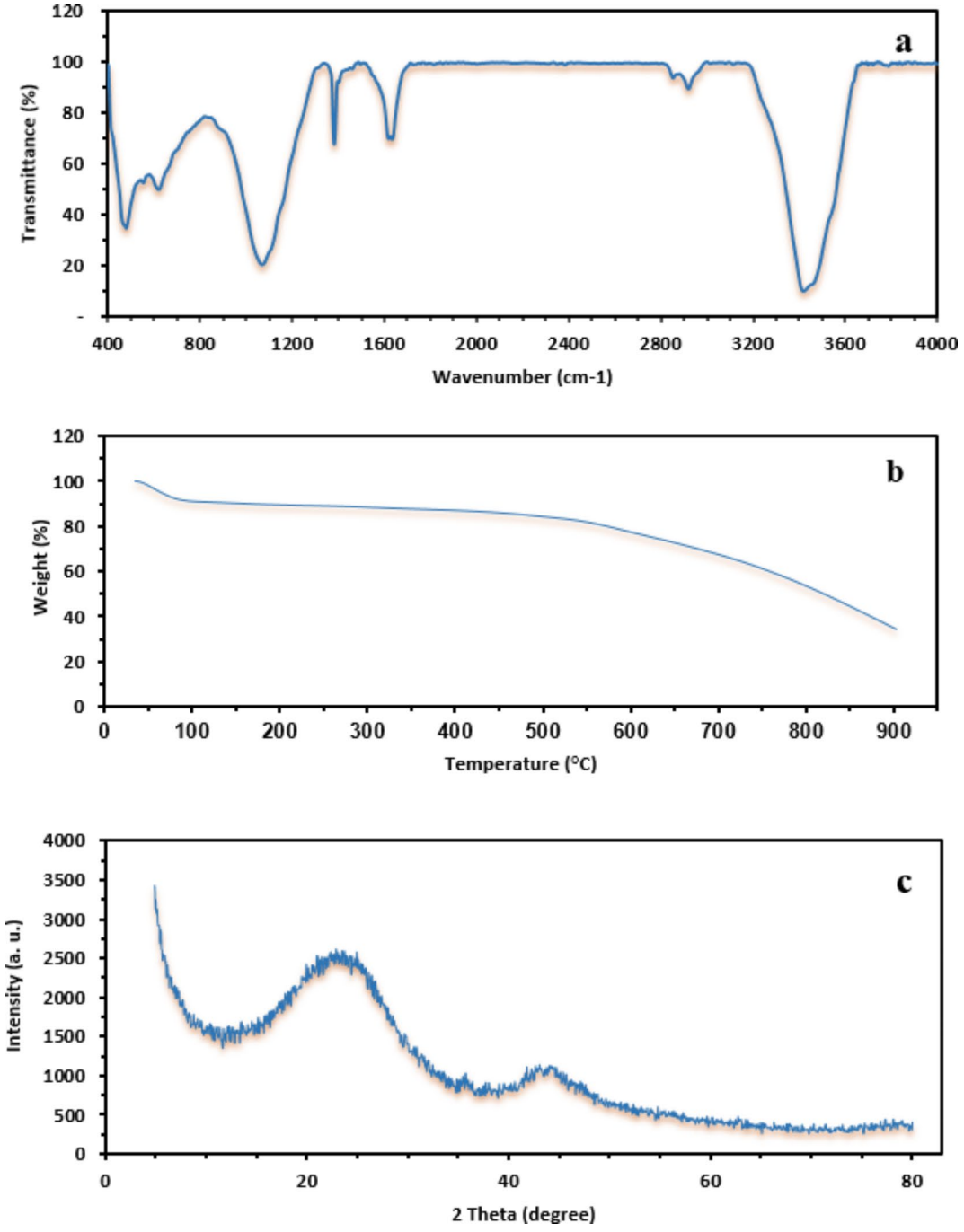

Fig. 2. (**a**) FTIR spectra of BW-AC (**b**) TGA of BW-AC (**c**) XRD pattern of BW-AC.

where A, B, C and D define the adsorbent dosage, pH, OTC initial concentration, and contact time, respectively. The coefficients of the parameters given in the equation above describe the importance of each parameter. Additionally, Pareto analysis was applied to indicate the percentage effect of different parameters (P_i) in order to identify the most effective and least significant parameters[63]:

$$P_i = \left(\frac{\beta_i^2}{\sum \beta_i^2}\right) \times 100 \quad (i \neq 0) \tag{4}$$

Based on the coefficients and the pareto chart shown in Fig. 5, initial concentration (C) was the most important parameter (49.7%) affecting the capacity of BW-AC for OTC adsorption. The effects of other parameters on the adsorption results were 40.8% for adsorbent dosage, 47.9% for pH and 4.9% for contact time.

The accuracy of the quadratic model and the affecting parameters significance was determined using ANOVA. This method breaks down the total variation in a dataset into different parts linked to specific factors.

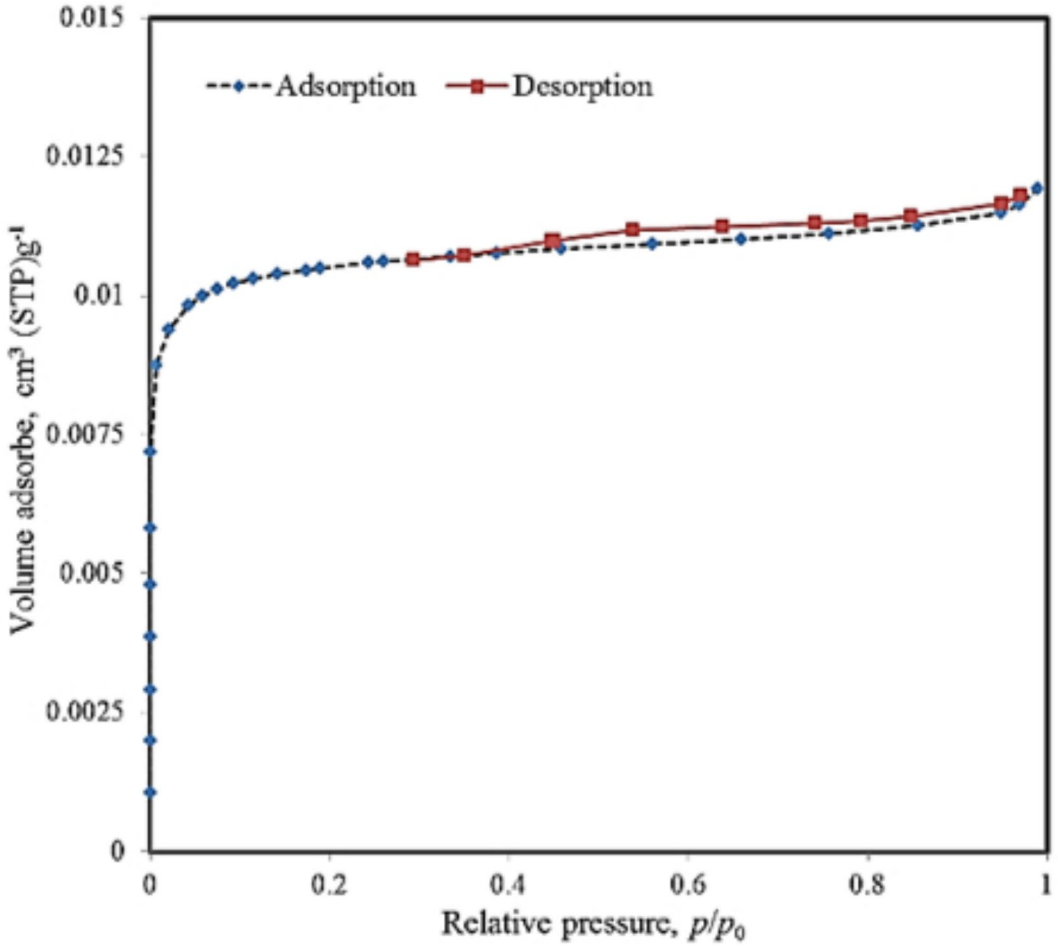

Fig. 3. N_2 adsorption–desorption isotherms of BW-AC at 77 K.

Precursor	Activating agent	SBET (m^2/g)	Mean pore diameter (nm)	Total pore volume (cm^3/g)	References
BW-AC	KOH	903.07	0.41	1.83	This study
Cones biomass of Iranian pine trees	K_2CO_3	1201.00	2.58	0.77	[57]
Cones biomass of Iranian pine trees	KOH	1116.00	2.23	0.65	[58]
Rubber fruit shells	$ZnCl_2$	456.00	3.44	NA	[59]
Vinasse waste from fermented sugar beet	NA	832.30	NA	0.45	[60]
Coffee waste	H_3PO_4	925.00	NA	0.71	[61]
Cacao shell	NA	85.00	2.70	0.05	[62]
Pinecone	KOH	1191.00	NA	NA	[55]
Vinasse waste of molasses-to-ethanol process	NA	989.00	NA	0.57	[53]

Table 3. BET Surface Area (SBET), total pore volume, and mean pore size of the adsorbents in similar studies. *NA* not available.

This helps in testing hypotheses about the parameters of the model[64]. The ANOVA results of the fitted model are given in Table 4. The high calculated F-value of 42.1 was more than the tabulated F-value at a significance level of 0.05, df = 14, and n = 30 (F0.05,14,16 = 2.37), so it can be concluded that the designed model has a high level of sufficiency for OTC adsorption. The P-values being less than 0.05 also indicate that the model and terms are significant[65]. Based on the ANOVA results, the parameters of A (adsorbent dosage), B (pH), C (initial concentration), and the quadratic terms including AA, AB, AC and BC were significant and other remaining terms were not. Based on the results indicated in Table 4, the R^2 value was 97.5%. The small difference between R^2 and R^2_{adj} (95.2%) implied a good fit between experimental data and predicted values of the quadratic model.

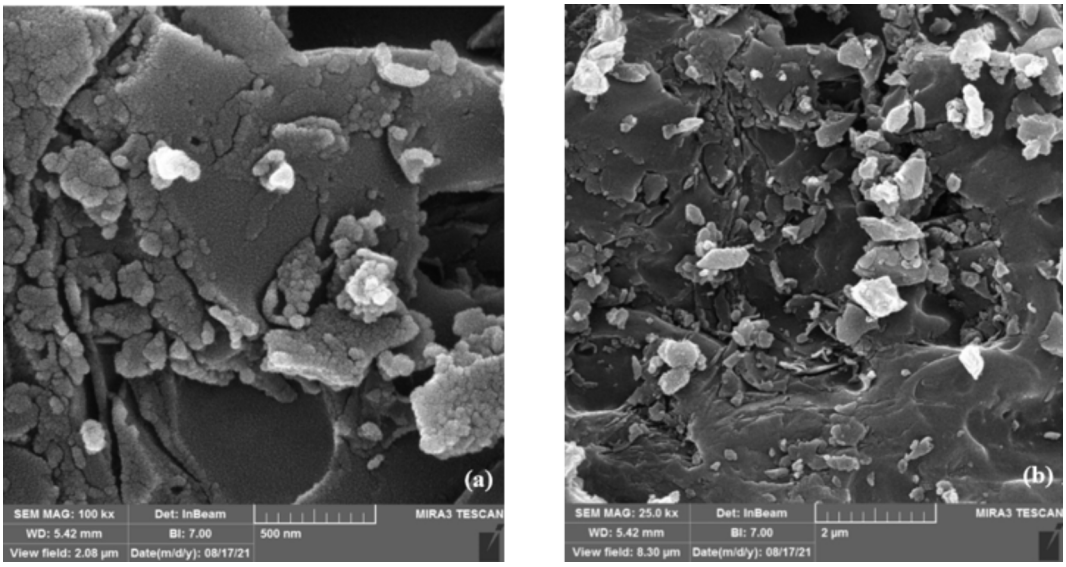

Fig. 4. SEM micrographs of activated carbon porous surface at (**a**) 100 Kx (**b**) 25 Kx magnification.

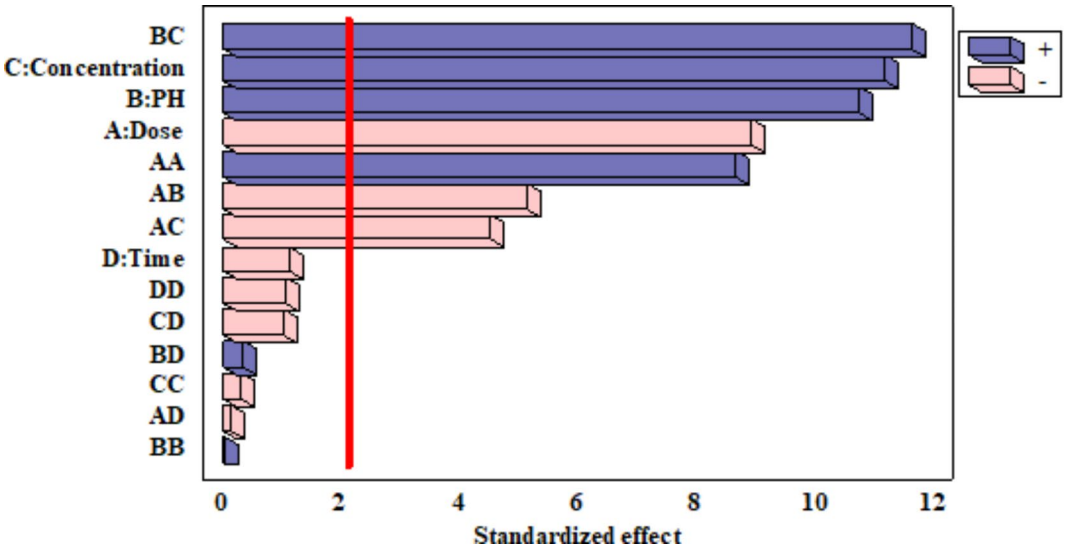

Fig. 5. Standardized Pareto Chart for OTC adsorption by BW-AC.

Response surface and contour plots of studied parameters

Figure 6 shows three-dimensional plots of studied parameters affecting the adsorption capacity of prepared BW-AC. The plots show the simultaneous effect of two parameters on the response factor while other variables were stabilized at certain levels, and the CCD-RSM was applied for evaluating these effects on OTC adsorption by BW-AC[66]. The impact of adsorbent dosage and solution pH on the adsorption capacity was examined in Fig. 6a and b. The study was conducted with a constant OTC concentration of 45 mg and a contact time of 35 min. It was found that increasing the pH of the solution had a positive effect on the adsorption capacity, with the highest capacity observed at pH 10. This enhancement can be attributed to the improved interaction between the functional groups on the adsorbent surface and the pollutant. At higher pH levels, the adsorbent surface becomes partially positively charged, leading to stronger attraction forces between the negatively charged OTC particles and the positively charged surface of the adsorbent. Additionally, hydrogen bonding between the positive NH_2 group and the adsorbent may occur. Conversely, at lower pH values, an increase in H_3O^+ions in the solution can reduce adsorption capacity by competing for active binding sites on the BW-AC surface. This competition may saturate the binding sites, making additional adsorbent dosage less effective and decreasing the overall adsorption capacity[67]. As shown in Fig. 6c and d, increasing the initial concentration of OTC led to a higher adsorption capacity at a fixed pH of 6.5 and contact time of 35 min. The increase in concentration improved adsorption by increasing the movement of pollutants to the binding sites. The combined impact of pH and initial concentration is illustrated in Fig. 6e and f. When the adsorbent dosage and contact time were kept

	Sum of squares	Df	Mean square	F-ratio	*P* value	
Model	69,809.8	14	4986.4	42.1	0.0001	Significant
A: Dosage	9493.10	1	9493.1	80.10	0.0000	
B: pH	13,751.10	1	13,751.1	116.03	0.0000	
C: Initial concentration	14,833.50	1	14,833.5	125.16	0.0000	
D: Time	146.10	1	146.1	1.23	0.2843	
AA	8933.60	1	8933.6	75.38	0.0000	
AB	3125.40	1	3125.4	26.37	0.0001	
AC	2417.20	1	2417.2	20.40	0.0004	
AD	2.10	1	2.1	0.02	0.8962	
BB	0.20	1	0.2	0.00	0.9704	
BC	16,078.20	1	16,078.2	135.66	0.0000	
BD	12.40	1	12.4	0.10	0.7509	
CC	9.80	1	9.8	0.08	0.7776	
CD	120.60	1	120.6	1.02	0.3292	
DD	129.20	1	129.2	1.09	0.3130	

Table 4. ANOVA of the quadratic model for OTC adsorption.

constant at 27.5 mg and 35 min, the adsorption capacity increased with higher pH and initial concentration. Although the effect of contact time on q_e was not significant, it was observed that OTC adsorption on BW-AC decreased during the experiment due to saturation of the adsorbent's active sites in the final few minutes.

Optimization of OTC adsorption process

The study utilized an experimental design to determine the best values for key factors in order to achieve the highest possible response factor in the experiment[68]. Traditional methods for optimization involved numerous trials, which were time-consuming, challenging, and required a large amount of chemicals. However, the CCD-RSM optimization method significantly reduces the number of experiments needed to identify the optimal conditions. In this research, solutions with the highest adsorption capacity were examined, and the optimal values for the influencing parameters were determined using a numerical CCD-based optimization program, Statgraphics. Table 5 in this study presents the observed optimal parameter values that impact the adsorption of OTC.

Adsorption isotherms

Adsorption isotherms are applicable for defining the behavior of pollutants and adsorbents in the equilibrium process by estimating the adsorbate distribution between solid/solution phases. Different adsorption isotherms can be applied for adsorption equilibrium data analysis. In this study, Langmuir, Freundlich, Redlich-Peterson and Dubinin–Radushkevich isotherm models were used to find the best-fitted correlation in the equilibrium curves. The equations of these isotherms are given in Table 6[69]. However, the linear fitting curves of the OTC adsorption isotherms are not displayed.

The Langmuir isotherm defines homogeneous sites on the surface that are equally active for monolayer adsorption, the adsorption energy is constant and equal in all sites, and the adsorbent molecules are fixed at its surface[70]. The isotherm parameters were calculated from isotherm plots shown in Fig. 7 and summarized in Table 2. The maximum adsorption capacity of OTC on BW-AC was 500 mg/g, based on the Langmuir isotherm. The separation factor (R_L) is an important constant of Langmuir isotherm that specifies the isotherm characteristics, and it can be used to investigate if the adsorption process is unfavorable $(R_L > 1)$, linear $(R_L = 1)$, favorable $(0 < R_L < 1)$ or irreversible $(R_L = 0)$. In this study, all the R_L values were between 0.64 and 0.96, showing that the OTC adsorption on BW-AC was favorable. The Freundlich isotherm is an empirical equation that describes a multi-layer adsorption on a heterogeneous surface. In this model, the addition of pollutant concentration increases the adsorption due to the interaction between the adsorbed molecules. Based on the values given in Table 2, the R^2 value of the Langmuir and Freundlich isotherms are 0.95 and 0.99, respectively. Therefore, it can be said that the Freundlich isotherm is more adequate to describe the adsorption of OTC on BW-AC and there is a good fit between the analysis data and the isotherm. For the adsorption process clarification, after the attachment of pollutants to more active binding sites, the attachment rate will be decreased because of occupation of the binding sites. Also, the amount of (n) parameter in the Freundlich equation indicates whether the adsorption is linear (n = 1), whether it is a chemical process (n < 1), or whether it is a physical process (n > 1). The value of n = 1.25 indicates that the physical process is favorable for the BW-AC adsorption system. The Redlich-Peterson isotherm is a three-parameter equation where $K_{RP}\,(L/g)$ and $\alpha\,(L/mg)^{\beta}$ are the isotherm constants and β is the parameter that lies between 0 and 1. When β approaches 1, the Redlich-Peterson model transforms to the Langmuir isotherm whereas when β approaches 0, the Redlich-Peterson equation converts to Henry's law equation and the Freundlich isotherm would be more suitable for defining the adsorption system. As shown in Table 7, β is 0.23 in this experiment, showing that the Freundlich isotherm is preferable for the system. The Dubinin–Radushkevich isotherm is usually used to define the mechanism of the adsorption on a heterogeneous surface with a Gaussian energy distribution[71]. Following the Dubinin–Radushkevich equation

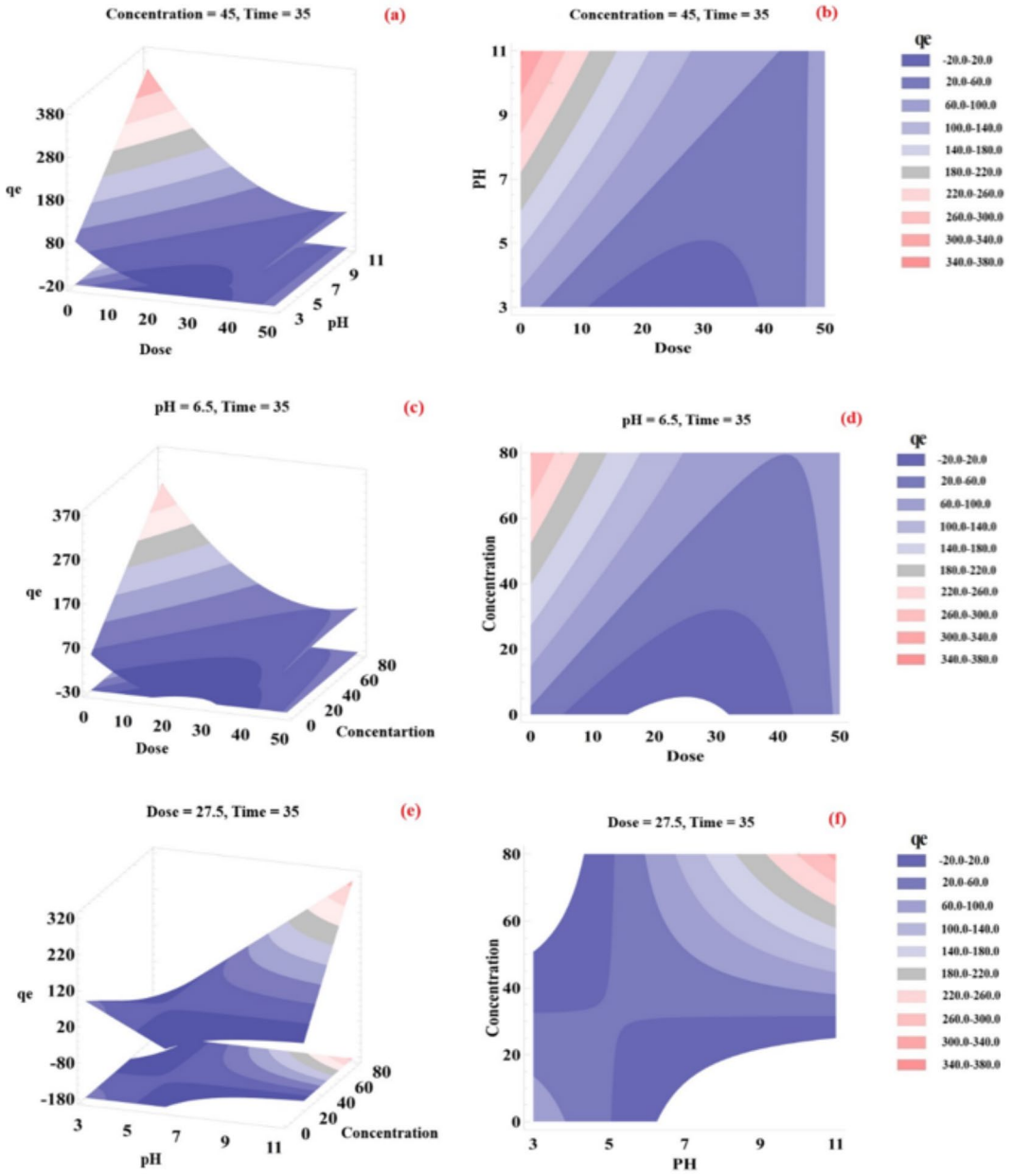

Fig. 6. 3-D response surface graphs for combined effects of (**a** and **b**) adsorbent dosage and pH, (**c** and **d**) adsorbent dosage and initial concentration, and (**e** and **f**) initial concentration and pH on adsorption of OTC by BW-AC.

	Adsorbent dosage (mg)	pH	Initial concentration (mg/L)	Contact time (min)
BW-AC	16.25	8.25	62.50	23.46

Table 5. Optimization of vital parameters based on the response surface modeling.

shown in Table 6, the plot of $\ln q_e$ versus ε^2 was drawn and the constants of E and q_s were obtained from slope and intercept, respectively. The mean free energy (E) of sorption per mole of the sorbate as it is transferred to the surface of the solid from an infinite distance in the solution indicates whether the adsorption is physical (E < 8 kJ/mol), or the adsorption is chemical $(8 < E < 16\ kJ/mol)$, or whether the adsorption type is intra-particle diffusion adsorption (E > 16 kJ/mol). As shown in Table 7, the E value was 0.31 confirming the physical nature of OTC adsorption on BW-AC.

Langmuir	$C_e/q_e = 1/(K_L\ q_e) + C_e/Q_0$
	$R_L = 1/(1 + K_L\ C_0)$
Freundlich	$\ln q_e = 1/n\ \ln C_e + \ln K_F$
Redlich–Peterson	$C_e/q_e = 1/K_{RP} + \alpha/K_{RP}\ C_e\hat{}\beta$
Dubinin–Radushkevich	$\ln q_e = \ln q_s - \beta_{DR}\varepsilon\hat{}2$
	$\varepsilon = RT\ \ln(1 + 1/C_e)$
	$E = (1/\sqrt{(2\beta_{DR})})$

Table 6. The linear forms of isotherm models. Q_0 = maximum adsorption capacity; K_L = Langmuir constant; R_L = separation factor; K_F, n = Freundlich constants; K_{RP}, α, β = Redlich–Peterson constants; β_{DR} = Dubinin–Radushkevich constant, E = mean free energy.

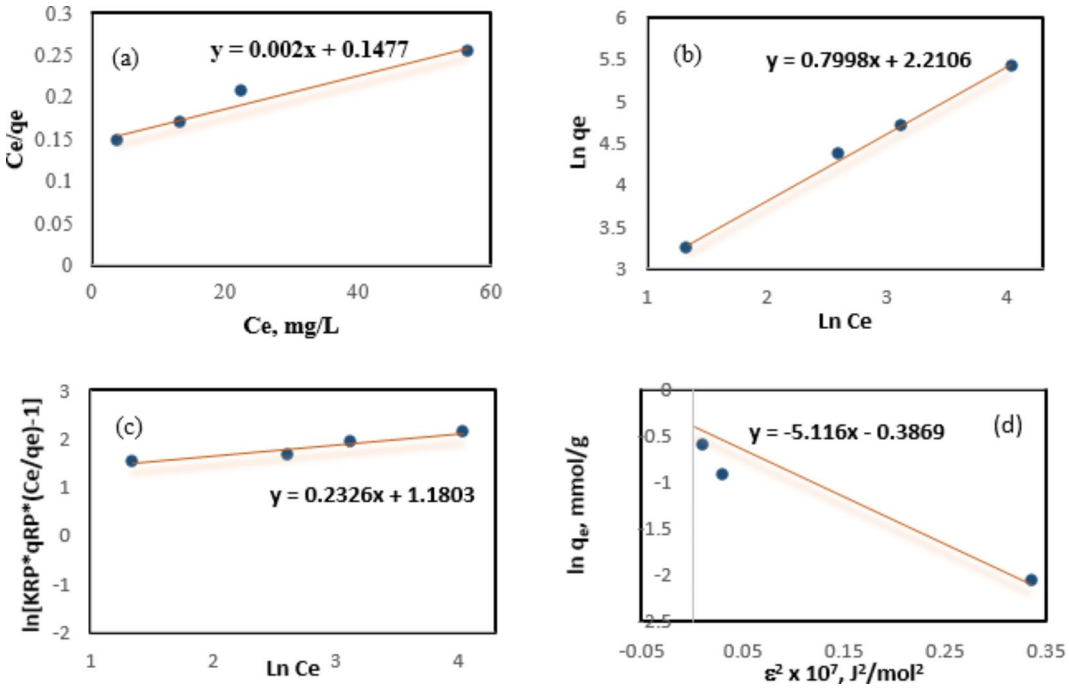

Fig. 7. (**a**) Langmuir (**b**) Freundlich (**c**) Redlich–Peterson (**d**) Dubinin–Radushkevich isotherm plots for OTC adsorption on BW-AC.

Comparison with other adsorbents

Table 8 presents a comparison of the maximum adsorption capacity of BW-AC and other adsorbents used in previous studies for OTC removal. The results show that BW-AC has a significantly higher uptake capacity compared to other adsorbents. This can be attributed to the presence of effective functional groups and a greater number of active sites on the high surface area of BW-AC, which enhance its ability to adsorb OTC. The superior adsorption capacity of BW-AC suggests its potential as an efficient adsorbent for removing OTC from wastewater.

Thermodynamics

Thermodynamic studies were carried out under optimized conditions including time, initial concentration, pH, and adsorbent dosage. A 100 ml solution was employed under these optimized parameters, with the sole variation being the temperature, which was adjusted to 288 K, 298 K, 308 K, and 318 K for the experimental study. Thermodynamic studies are necessary to determine the adsorption characteristics and behavior of the isolated system behavior. The Gibbs free energy change (ΔG°), enthalpy change (ΔH°) and entropy change (ΔS°) were calculated from the following Gibbs free energy equations:

$$K_C = C_{Ad}/C_e \tag{5}$$

$$\Delta G^\circ = -RT\ \ln K_C \tag{6}$$

$$\ln K_C = (\Delta S^\circ)/R - (\Delta H^\circ)/RT \tag{7}$$

Langmuir			Freundlich			Redlich–Peterson			Dubinin–Radushkevich			
q_m	K_L	R^2	K_F	n	R^2	K_{RP}	β	R^2	q_s	β_{DR}	E	R^2
500.00	0.01	0.95	9.12	1.25	0.99	3.26	0.23	0.95	155.60	5.12	0.31	0.83

Table 7. Adsorption isotherm parameters for OTC adsorption on BW-AC.

Adsorbents	Adsorption conditions	Adsorption capacity (mg/g)	References
Barley wastes activated carbon (BW-AC)	pH 8.25, adsorbent dosage 162.5 mg/L, initial concentration 62.5 mg/L, temperature 25°C	500	This study
Uncalcined nanohydroxyapatite (HA-uc)	pH 8, adsorbent dosage 2000 mg/L, initial concentration 50 mg/L, temperature 20°C	291	[72]
Multiwalled carbon nanotubes (MWNT10)	pH 7, adsorbent dosage 25,000 mg/L, initial concentration 2.5 mg/L, temperature 23°C	190	[73]
Surfactant-modified alumina (SMA)	pH 4, adsorbent dosage 25,000 mg/L, initial concentration 10^{-4} M, temperature 25°C	143	[74]
Magnetic microspheres with bimetal oxide shell (Mag@ZnO–Co_3O_4)	pH 7, adsorbent dosage 250 mg/L, initial concentration of 10 mg/L, temperature 25°C	128	[75]

Table 8. Comparison of different adsorbents for OTC adsorption.

		ΔG° (KJ/mol)				
ΔH° (KJ/mol)	ΔS° (KJ/mol k)	288	298	308	318	R^2
13.01	0.05	− 1.99	− 2.52	− 3.04	− 3.56	0.99

Table 9. Thermodynamic parameters of OTC adsorption on BW-AC at different temperatures (in K).

where K_C is the equilibrium constant, C_{Ad} is the adsorbed OTC concentration at equilibrium (mg/L), C_e is the OTC equilibrium concentration in the solution (mg/L), R is the universal gas constant (8.314 J/mol k), T is the solution temperature (K) and K_C (L/mg) is the Langmuir isotherm constant. The values of ΔH° and ΔS° can be derived from the slope and intercept of the Van't Hoff plot of $\ln K_C$ versus 1/T. The obtained values of ΔH°, ΔS° and ΔG° for adsorption of OTC on BW-AC adsorbent are indicated in Table 9.

The positive ΔH° value indicates an endothermic adsorption process, and increasing the temperature will increase the adsorption of OTC due to viscosity decrement of the solution. Therefore, a better distribution of pollutant particles over internal pores and binding sites of the adsorbent would be obtained. The positive value of ΔS° indicates that randomness on the adsorbent interface with OTC particles in the system was increased, so a better binding between the OTC particles and BW-AC sites would be achieved. The negative value of ΔG° shows feasibility and a spontaneous physiosorption nature of OTC adsorption process at specified temperatures being studied for all concentrations. Also, decrement of ΔG° with increasing temperature indicates that the adsorption was more spontaneous at higher temperatures.

Conclusion

In this study, the adsorption capacity of BW-AC for OTC antibiotic adsorption in aqueous solutions was investigated. The prepared adsorbent was characterized and high specific surface area with multiple activated adsorption sites was observed. The CCD-RSM was applied to optimize the vital parameters affecting the adsorption capacity in a single system. As a result of statistical analysis, the optimum values of the studied parameters of adsorbent dosage, pH, OTC initial concentration and contact time were 16.25 (mg), 8.25, 62.50 (mg/L) and 23.46 (min), respectively. The Langmuir, Freundlich, Redlich-Peterson, and Dubinin–Radushkevich isotherms were studied and the experimental data were best fitted to the Freundlich model with a high correlation coefficient (R^2 0.99) for OTC adsorption. Thermodynamic studies showed that the adsorption process was endothermic and spontaneous. Taking into consideration the results above, the activated carbon adsorbent synthesized from barley wastes has an impressive potential for efficient adsorption of OTC from wastewater. The use of CCD-RSM and application of BW-AC for the removal of OTC from aqueous solutions has not been previously investigated, and this study is therefore original in this respect.

Data availability

All data generated or analyzed during this study are included in this study.

Received: 28 November 2023; Accepted: 13 September 2024
Published online: 07 October 2024

References

1. Mycologia, S. W. *What is an Antibiotic or an Antibiotic Substance?* (Taylor & Francis, 1947).
2. Hasani, K., Peyghami, A., Moharrami, A., Vosoughi, M. & Dargahi, A. The efficacy of sono-electro-Fenton process for removal of Cefixime antibiotic from aqueous solutions by response surface methodology (RSM) and evaluation of toxicity of effluent by microorganisms. *Arab. J. Chem.* **13**, 6122–6139 (2020).
3. Seid-Mohammadi, A. & Ghorbanian, Z. Photocatalytic degradation of metronidazole (MnZ) antibiotic in aqueous media using copper oxide nanoparticles activated by H_2O_2/UV process. *Desalin. Water Treat.* https://doi.org/10.5004/dwt.2020.25772 (2020).
4. Homem, V. & Santos, L. Degradation and removal methods of antibiotics from aqueous matrices: A review. *J. Environ. Manag.* **92**, 2304–2347 (2011).
5. Michalova, E., Novotna, P. & Schlegelova, J. Tetracyclines in veterinary medicine and bacterial resistance to them. *Vet. Med.* **49**, 79–100 (2004).

6. Seidmohammadi, A., Vaziri, Y., Dargahi, A. & Nasab, H. Z. Improved degradation of metronidazole in a heterogeneous photo-Fenton oxidation system with PAC/Fe_3O_4 magnetic catalyst: Biodegradability, catalyst specifications, process optimization, and degradation pathway. *Biomass Convers. Biorefin.* **13**, 9057–9073 (2023).
7. Gao, P., Ding, Y. & Li, H. Occurrence of pharmaceuticals in a municipal wastewater treatment plant: Mass balance and removal processes. *Chemosphere* **88**, 17–24 (2012).
8. Pan, X., Qiang, Z., Ben, W. & Chen, M. Residual veterinary antibiotics in swine manure from concentrated animal feeding operations in Shandong Province, China. *Chemosphere* **84**, 695–700 (2011).
9. Danner, M. & Robertson, A. Antibiotic pollution in surface fresh waters: Occurrence and effects. *Sci. Total Environ.* **664**, 793–804 (2019).
10. Pacheco, C. V. G. *et al.* Degradation of tetracyclines in different water matrices by advanced oxidation/reduction processes based on gamma radiation. *J. Chem. Technol. Biotechnol.* **88**, 1096–1108 (2013).
11. Hernández, F., Sancho, J. & Ibáñez, M. Antibiotic residue determination in environmental waters by LC-MS. *TrAC Trends Anal. Chem.* **26**, 466–485 (2007).
12. Sponza, D. T. & Çelebi, H. Removal of oxytetracycline (OTC) in a synthetic pharmaceutical wastewater by sequential anaerobic multichamber bed reactor (AMCBR)/completely stirred tank reactor (CSTR) system: Biodegradation and inhibition kinetics. *J. Chem. Technol. Biotechnol.* **87**, 961–975 (2012).
13. Christian, T. *et al.* Determination of antibiotic residues in manure, soil, and surface waters. *Acta Hydrochim. Hydrobiol.* **31**, 36–44 (2003).
14. Göbel, A., Thomsen, A., McArdell, C. S., Joss, A. & Giger, W. Occurrence and sorption behavior of sulfonamides, macrolides, and trimethoprim in activated sludge treatment. *Environ. Sci. Technol.* **39**, 3981–3989 (2005).
15. Chemosphere, K. K. *Antibiotics in the Aquatic Environment: A Review–Part I* (Elsevier, 2009).
16. Ding, C. & He, J. Effect of antibiotics in the environment on microbial populations. *Appl. Microbiol. Biotechnol.* **87**, 925–941 (2010).
17. Larsson, D. J. Antibiotics in the environment. *Upsala J. Med. Sci.* **119**, 108–112 (2014).
18. Daghrir, R. & Drogui, P. Tetracycline antibiotics in the environment: A review. *Environ. Chem. Lett.* **11**, 209–227 (2013).
19. Seid-Mohammadi, A., Asgarai, G., Ghorbanian, Z. & Dargahi, A. The removal of cephalexin antibiotic in aqueous solutions by ultrasonic waves/hydrogen peroxide/nickel oxide nanoparticles (US/H_2O_2/NiO) hybrid process. *Sep. Sci. Technol. (Phila.)* **55**, 1558–1568 (2020).
20. Perry, D., Amaranthus, M. & Borchers, J. Bootstrapping in ecosystems. *JSTOR* https://doi.org/10.2307/1311159 (1989).
21. Pickens, L. & Chemistry, Y. T. Oxytetracycline biosynthesis. *J. Biol. Chem.* **285**, 27509–27515 (2010).
22. Sczesny, S., Nau, H. & Hamscher, G. Residue analysis of tetracyclines and their metabolites in eggs and in the environment by HPLC coupled with a microbiological assay and tandem mass spectrometry. *J. Agric. Food Chem.* **51**, 697–703 (2003).
23. Çelebi, H. & Gök, O. Removals of non-analogous OTC and BaP in AMCBR with and without primary substrate. *Environ. Technol.* **37**, 1768–1781 (2017).
24. Miranda, C. Bacterial resistance to oxytetracycline in Chilean salmon farming. *Aquaculture* **212**, 31–47 (2002).
25. Gallo, A. *et al.* Oxytetracycline induces DNA damage and epigenetic changes: A possible risk for human and animal health?. *PeerJ* **5**, e3236 (2017).
26. Li, D. *et al.* Determination and fate of oxytetracycline and related compounds in oxytetracycline production wastewater and the receiving river. *Environ. Toxicol. Chem.* **27**, 80–86 (2008).
27. Aga, D., O'Connor, S. & Ensley, S. Determination of the persistence of tetracycline antibiotics and their degradates in manure-amended soil using enzyme-linked immunosorbent assay and liquid. *J. Agric. Food Chem.* **53**, 7165–7171 (2005).
28. Gothwal, R. & Shashidhar, T. Antibiotic pollution in the environment: A review. *Clean (Weinh)* **43**, 479–489 (2015).
29. Adams, C., Wang, Y., Loftin, K. & Meyer, M. Removal of antibiotics from surface and distilled water in conventional water treatment processes. *J. Environ. Eng.* **128**, 253–260 (2002).
30. Li, B. Biodegradation and adsorption of antibiotics in the activated sludge process. *Environ. Sci. Technol.* **44**, 3468–3473 (2010).
31. Nayeri, D. & Mousavi, S. Oxytetracycline removal from aqueous solutions using activated carbon prepared from corn stalks. *J. Appl. Res. Water Wastewater* **6**, 67–72 (2019).
32. Li, K. *et al.Ozonation of Oxytetracycline and Toxicological Assessment of Its Oxidation By-Products* (Elsevier).
33. Huang, L. *et al.Comparative Study on Characterization of Activated Carbons Prepared by Microwave and Conventional Heating Methods and Application in Removal of Oxytetracycline* (Elsevier).
34. Tan, I. & Ahmad, A. Adsorption isotherms, kinetics, thermodynamics and desorption studies of 2, 4, 6-trichlorophenol on oil palm empty fruit bunch-based activated carbon. *J. Hazard. Mater.* **164**, 473–482 (2009).
35. Pourali, P. *et al.* Loading of zinc oxide nanoparticles from green synthesis on the low cost and eco-friendly activated carbon and its application for diazinon removal: Isotherm, kinetics and retrieval study. *Appl. Water Sci.* **13** (2023).
36. Dargahi, A., Samarghandi, M. R., Shabanloo, A., Mahmoudi, M. M. & Nasab, H. Z. Statistical modeling of phenolic compounds adsorption onto low-cost adsorbent prepared from aloe vera leaves wastes using CCD-RSM optimization: Effect of parameters, isotherm, and kinetic studies. *Biomass Convers. Biorefin.* **13**, 7859–7873 (2023).
37. Wang, L. *et al.Adsorption of 2, 4-Dichlorophenol on Mn-Modified Activated Carbon Prepared from Polygonum Orientale Linn* (Elsevier).
38. Sun, Y. *et al.Preparation of Highly Developed Mesoporous Activated Carbon by H4P2O7 Activation and Its Adsorption Behavior for Oxytetracycline* (Elsevier).
39. Xu, H. *et al.* Nanoporous activated carbon derived from rice husk for high performance supercapacitor. *J. Nanomater.*
40. Almasi, A. & Mousavi, S. Walnut shell as a natural adsorbent for the removal of reactive red 2 form aqueous solution. *J. Appl. Basic Sci.* **10**, 551–556 (2016).
41. Almasi, A., Navazeshkha, F. & Mousavi, S. A. Biosorption of lead from aqueous solution onto Nasturtium officinale: Performance and modeling. *Desalin. Water Treat.* https://doi.org/10.5004/dwt.2017.20308 (2017).
42. Lua, A. & Lau, F. Influence of pyrolysis conditions on pore development of oil-palm-shell activated carbons. *J. Anal. Appl. Pyrolysis* **76**, 96–102 (2006).
43. Balarak, D., Mostafapour, F. K., & Azarpira, H. Adsorption kinetics and equilibrium of ciprofloxacin from aqueous solutions using Corylus avellana (Hazelnut) activated carbon- Google Scholar.
44. Mohammadi, M. *et al.* Optimizing biological treatment of petroleum industry wastewater in a facultative stabilization pond for simultaneous removal of carbon and phenol. *Toxin Rev.* **40**, 189–197 (2021).
45. Samarghandi, M. R. *et al.* Application of a fluidized three-dimensional electrochemical reactor with Ti/SnO_2–Sb/β-PbO_2 anode and granular activated carbon particles for degradation and mineralization of 2,4-dichlorophenol: Process optimization and degradation pathway. *Chemosphere* **279**, 130640 (2021).
46. Heidari, M., Vosoughi, M., Sadeghi, H., Dargahi, A. & Mokhtari, S. A. Degradation of diazinon from aqueous solutions by electro-Fenton process: Effect of operating parameters, intermediate identification, degradation pathway, and optimization using response surface methodology (RSM). *Sep. Sci. Technol.* **56**, 2287–2299 (2021).
47. Molla Mahmoudi, M., Khaghani, R., Dargahi, A. & Monazami Tehrani, G. Electrochemical degradation of diazinon from aqueous media using graphite anode: Effect of parameters, mineralisation, reaction kinetic, degradation pathway and optimisation using central composite design. *Int. J. Environ. Anal. Chem.* **102**, 1709–1734 (2022).

48. Dargahi, A., Vosoughi, M., Ahmad Mokhtari, S., Vaziri, Y. & Alighadri, M. Electrochemical degradation of 2,4-dinitrotoluene (DNT) from aqueous solutions using three-dimensional electrocatalytic reactor (3DER): Degradation pathway, evaluation of toxicity and optimization using RSM-CCD. *Arab. J. Chem.* **15** (2022).
49. Song, X. *et al.* Adsorption mechanisms and the effect of oxytetracycline on activated sludge. *Bioresour. Technol.* **151**, 428–431 (2014).
50. Alghamdi, A. A. *et al.* Efficient adsorption of lead(II) from aqueous phase solutions using polypyrrole-based activated carbon. *Materials* https://doi.org/10.3390/ma12122020 (2020).
51. Krahnstöver, T. & Plattner, J. Quantitative detection of powdered activated carbon in wastewater treatment plant effluent by thermogravimetric analysis (TGA). *Water Res.* **101**, 510–518 (2016).
52. Girgis, B., Temerk, Y. & Gadelrab, M. X-ray diffraction patterns of activated carbons prepared under various conditions. *Carbon Lett.* **8**, 95–100 (2007).
53. Wu, F., Tseng, R. & Hu, C. Comparisons of pore properties and adsorption performance of KOH-activated and steam-activated carbons. *Microporous Mesoporous Mater.* **80**, 95–106 (2005).
54. Sing, K. S. W. *et al.* Reporting physisorption data for gas/solid systems with special reference to the determination of surface area and porosity. *Pure Appl. Chem.* **57**, 603–619 (1985).
55. Abdedayem, A., Guiza, M. & Ouederni, A. Copper supported on porous activated carbon obtained by wetness impregnation: Effect of preparation conditions on the ozonation catalyst's characteristics. *C. R. Chim.* **18**, 100–109 (2015).
56. Tansel, B. & Nagarajan, P. SEM study of phenolphthalein adsorption on granular activated carbon. *Adv. Environ. Res.* **8**, 411–415 (2004).
57. Valizadeh, S., Younesi, H. & Bahramifar, N. Highly mesoporous K2CO3 and KOH/activated carbon for SDBS removal from water samples: Batch and fixed-bed column adsorption process. *Environ. Nanotechnol. Monit. Manag.* **6**, 1–13 (2016).
58. Suhdi, S.-C.W. Fine activated carbon from rubber fruit shell prepared by using $ZnCl_2$ and KOH activation. *Appl. Sci.* https://doi.org/10.3390/app11093994 (2021).
59. Kazak, O., Eker, Y. & Bingol, H. Novel preparation of activated carbon by cold oxygen plasma treatment combined with pyrolysis. *Chem. Eng. J.* **325**, 564–575 (2017).
60. Reffas, A., Bernardet, V. & David, B. Carbons prepared from coffee grounds by H_3PO_4 activation: Characterization and adsorption of methylene blue and Nylosan Red N-2RBL. *J. Hazard. Mater.* **175**, 779–788 (2010).
61. Ahmad, F., Daud, W. & Ahmad, M. Cocoa (*Theobroma cacao*) shell-based activated carbon by CO_2 activation in removing of Cationic dye from aqueous solution: Kinetics and equilibrium studies. *Chem. Eng. Res. Des.* **90**, 1480–1490 (2012).
62. Kazak, O., Eker, Y. & Bingol, H. Preparation of activated carbon from molasses-to-ethanol process waste vinasse and its performance as adsorbent material. *Bioresour. Technol.* **241**, 1077–1083 (2017).
63. Anupam, K., Dutta, S. & Bhattacharjee, C. Adsorptive removal of chromium(VI) from aqueous solution over powdered activated carbon: Optimisation through response surface methodology. *Chem. Eng. J.* **173**, 135–143 (2011).
64. Tripathi, P. & Srivastava, V. Optimization of an azo dye batch adsorption parameters using Box–Behnken design. *Desalination* **249**, 1273–1279 (2009).
65. Khuri, A. & Cornell, J. *Response Surfaces: Designs and Analyses* (2018).
66. Kalavathy, H. *et al.* Modelling, analysis and optimization of adsorption parameters for H_3PO_4 activated rubber wood sawdust using response surface methodology (RSM). *Colloids Surf. B Biointerfaces* **70**, 35–45 (2009).
67. Hasan, S., Ghosh, T. K., Viswanath, D. S., Loyalka, S. K. & Sengupta, B. Preparation and evaluation of fullers earth beads for removal of Cesium from waste streams. *Sep. Sci. Technol.* **42**, 717–738 (2007).
68. Arabkhani, P., Javadian, H. & Asfaram, A. A reusable mesoporous adsorbent for efficient treatment of hazardous triphenylmethane dye wastewater: RSM-CCD optimization and rapid microwave-assisted. *Sci. Rep.* https://doi.org/10.1038/s41598-021-02213-2 (2021).
69. Langmuir, I. The adsorption of gases on plane surfaces of glass, mica and platinum. *J. Am. Chem. Soc.* **40**, 1361–1403 (1918).
70. Samarghandi, M. R., Asgari, G., Shokoohi, R., Dargahi, A. & Arabkouhsar, A. Removing amoxicillin antibiotic from aqueous solutions by *Saccharomyces cerevisiae* bioadsorbent: Kinetic, thermodynamic and isotherm studies. *Desalin. Water Treat.* **152**, 306–315 (2019).
71. Seidmohammadi, A. *et al.* A comparative study for the removal of methylene blue dye from aqueous solution by novel activated carbon based adsorbents. *Progress Color Color. Coat.* **12**, 133–144 (2019).
72. Harja, M. & Ciobanu, G. Studies on adsorption of oxytetracycline from aqueous solutions onto hydroxyapatite. *Sci. Total Environ.* **628–629**, 36–43 (2018).
73. Oleszczuk, P., Pan, B. & Xing, B. Adsorption and desorption of oxytetracycline and carbamazepine by multiwalled carbon nanotubes. *Environ. Sci. Technol.***43**, 9167–9173 (2009).
74. Pham, T. D. *et al.* Adsorption characteristics of molecular oxytetracycline onto alumina particles: The role of surface modification with an anionic surfactant. *J. Mol. Liq.* **287**, 110900 (2019).
75. Lian, L., Lv, J. & Lou, D. Synthesis of novel magnetic microspheres with bimetal oxide shell for excellent adsorption of oxytetracycline. *ACS Sustain. Chem. Eng.* **5**, 10298–10306 (2017).

Acknowledgements

The authors are gratefully thankful to Dr. Zahra Sahebi the head of Arvin Zist Pooya lab for her collaboration in the laboratory analysis.

Author contributions

A.K.: Investigation, Supervision, Data curation, Writing-Original draft preparation, Project administration, Review and Editing. E.E.: Data analyzing, Laboratory experiments, Taking pictures in the lab and making the Fig. 1. F.G.: Methodology. M.E., F.E., and M.M.: Review and Editing, Laboratory experiments.

Funding

The authors declare that they have received no funding to financially support this study.

Declarations

Competing interests

The authors declare no competing interests.

Additional information

Correspondence and requests for materials should be addressed to A.K.